Pitching Motion Control of Underwater Traveling LSM Vehicle ME02 Using Controlled Air-Cored Electromagnet

K. Yoshida, M. El-Nemr, Y. Yamashita
Graduate School of Information Science and Electrical Engineering
Kyushu University
10-1 6-chome Hakozaki, Higashi-ku, Fukuoka, 812-8581
JAPAN
http://eesmain.ees.kyushu-u.ac.jp/~yoshida/yoshidae.html

Abstract: - When Marine Express starts to propel, an undesired pitching motion is established. In the attractive mode of operation, the propulsion and levitation forces produce additive torques and pitching motion becomes highly unstable. The current paper introduces enhanced control scheme for pitching motion of the underwater linear motor vehicle ME02 in attractive mode. Two air-cored electromagnets are utilized to produce damping torque. The proposed control technique successfully damped the pitching motion. In addition, the energy requirements of the new control system are much smaller than previous techniques. The simulation results show clearly that the new technique can be applied for real scale Marine Express.

Key-Words: - Linear Synchronous Motor Drive, Underwater Marine Express, Pitching Motion Control

1 Introduction

The Marine Express or Amphibious Maglev is a unique linear motor train able to run both on-land and underwater along the same guideway. This system would network on-land stations with offshore airports, basis or cities across the sea [1]. Due to Marine Express amphibious nature, its Maglev system would implement both attractive and repulsive operation modes to overcome the buoyancy forces under sea surface and gravity forces on-land respectively.

The second experimental model underwater vehicle (ME02) is a $1/25^{th}$ scale experimental model vehicle, which is used to show the experimental validity of underwater transportation system. However, its mass can be regulated to simulate experimentally both the attractive and repulsive modes of operation [2][3]. ME02 is 105cm long and 17cm in diameter. Fig.1 shows photography of ME02 vehicle while running underwater. It is levitated and propelled by the long-stator type permanent magnets linear synchronous motor (PM-LSM), which has the integrated function of linear synchronous motor propulsion and levitation. The combined propulsion and levitation is achieved via controlling "space vector" of LSM force. Propulsion and levitation are established by the motor resultant force components parallel and normal to the guideway in x-direction and z-direction respectively.

As the permanent magnets (PM) are arranged in alternating polarity along the vehicle, the working lines of the motors developed forces do not pass through the vehicle center of gravity. Thereby, resultant torque is established around the center of gravity and rotational motion around y-axis (pitching motion) is initiated. However, such pitching motion is undesired for vehicle operation. In addition, other disturbances like water flow, waves or undersea currents may also cause this undesirable motion. To achieve successful levitation, depending on the ratio of vehicle weight and buoyancy force, the LSM levitation force is controlled to be attractive or repulsive. However, for a real scale machine, the buoyancy forces would be much larger than vehicle weight. As it will be shown in the next section, in repulsive mode of operation, the pitching motion is naturally damped. On the other hand, in attractive mode, the pitching motion is highly unstable.

In previous studies, the pitching motion of ME02 was controlled in repulsive mode of operation by regulating the motor thrust force [3]. For highly unstable attractive mode, a single controlled electromagnet was utilized to compensate ME02 pitching torque and reduce the pitching motion [4]. In the current work, two air-cored controlled electromagnets (AEM) with fast acting controller are designed to control the pitching motion. The new control scheme has successfully damped pitching motion with smaller controller current,

Fig.1 Photography of ME02

hence with reduced power demand. In the next section, brief explanation of pitching motion would be introduced.

2 Pitching Motion Analysis for ME02

ME02 has three degrees of motion freedom namely propulsion, levitation and pitching motions. The guidance motion of ME02 is mechanically restricted for safety and other aspects. As mentioned before, the vehicle is a combined levitation and propulsion system with only one pair of armature coils and permanent magnets. However, it is technically very difficult to control motions of three degrees of freedom using only the thrust and lift forces in PM-LSM.

Beside the motor forces, the vehicle is mainly subjected to its weight and water buoyancy. When the vehicle moves horizontally, the torque produced by the buoyancy force is negligible because of very small horizontal distance between the vehicle center of gravity and center of buoyancy.

For practical Marine Express, to achieve magnetic levitation, when the buoyancy force is larger than the vehicle weight, the levitation forces is controlled to attract the vehicle to the guideway i.e. attractive mode of operation. Otherwise, when running on land, the levitation forces are controlled to repulse i.e. repulsive mode.

For both repulsive and attractive modes of operation, levitation forces will position the vehicle at standstill as illustrated in Fig.2 and Fig.3. The levitation forces produced by the most front and rear poles only are shown in Fig.2(a) and Fig.3(a) in repulsive and attractive modes, respectively. As the airgap length is equal for both poles, the developed forces are obviously equal and no pitching motion would be generated at standstill. When the motor starts to propel, the horizontal force components $F_{x,n}$ would generate resultant torque T_x and pitching motion is initiated. Thereby, the effective airgap of different poles would change and a resultant torque T_z is produced by the vertical components of the motor forces $F_{z,n}$. Where n is the pole number. The central pole has the number 1. The even and odd numbers are assigned to the poles on the right and left sides ascending away from the vehicle center. Hence, the pitching motion dynamic equation is given by:

$$\begin{aligned}(1+k_\phi)I_y\ddot{\phi} = &\sum_{v=0}^{7}F_{x,2v+1}(-d\cos\phi+v\tau\sin\phi)\\ &+\sum_{v=0}^{7}F_{z,2v+1}(d\sin\phi+v\tau\cos\phi)\\ &-\sum_{v=1}^{7}F_{x,2v}(d\cos\phi+v\tau\sin\phi)\\ &+\sum_{v=0}^{7}F_{z,2v}(d\sin\phi-v\tau\cos\phi)-F_{pR}\end{aligned} \quad (1)$$

where ϕ is pitching angle, k_ϕ is the virtual inertia coefficient around y-axis, I_y moment of inertial around y-axis

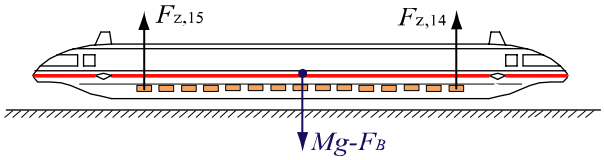

(a) At standstill

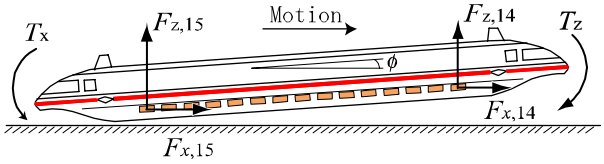

(b) During running

Fig. 2 Torque of PM-LSM in repulsive mode

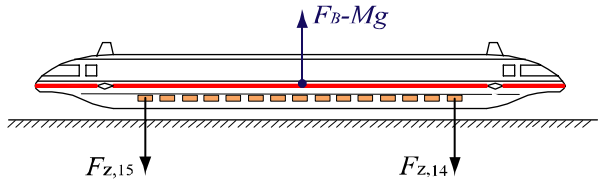

(a) At standstill

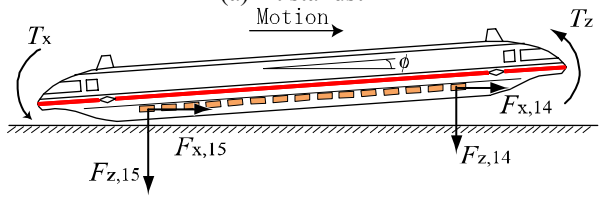

(b) During running

Fig.3 Torque of PM-LSM in attractive mode

and τ is the pole pitch. The revolving water resistance around y-axis is F_{pR}. Details of force calculation are found in [5].

The directions of torques T_x and T_z in repulsive and attractive modes are demonstrated in Fig.2(b) and Fig.3(b) respectively. It is clear that in attractive mode, torques are accumulative and highly unstable pitching motion results. Fortunately, for repulsive mode, the torque T_z is working against T_x. Therefore, T_z acts to damp the pitching motion. Therefore, efficient pitching motion control in attractive mode would be applicable for repulsive mode as well.

3 Air-Cored Controlled Electromagnet for Pitching Motion Control

In the current work, two air-cored electromagnets (AEM) are utilized to damp the pitching motion. As shown in Fig.4, the front and rear airgap lengths δ_F and δ_R are measured via laser sensors. The measured values are used to determine the average airgap required for the PM-LSM controller. In addition, these values are used to determine the current required for the front and rear air-cored controlled electromagnet coils. The current in both coils is determined according to the control law. To

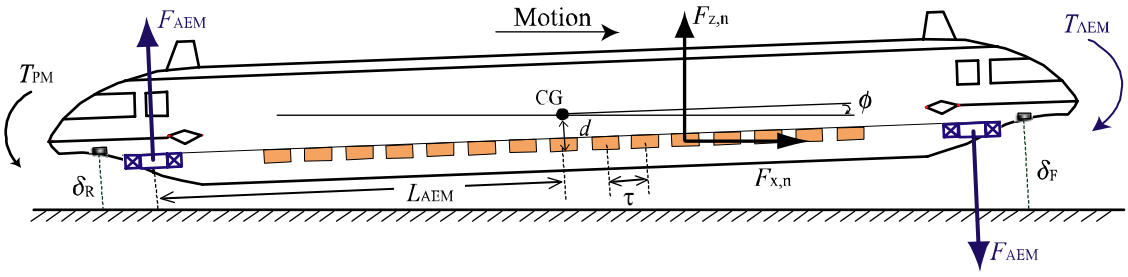

Fig.4 Pitching motion analysis model with two controlled AEM
(τ = 4.47cm, L_{AEM} = 44.7cm, d= 1cm)

synchronize pitching controller with the main servo controller of propulsion and levitation, the controlled electromagnets are placed in a multiple of pole pitch.

Based on the MVP transfer-matrix method proposed by the first author, the multilayer boundary-value field problem was solved and analytical expression for forces developed can be derived [5]. The thrust force F_{xAEM} developed by the AEM is found using the simple and exact final expressions:

$$F_{xAEM} = K_{F0} J_1 J_{C1} \tau \sin\frac{\pi}{\tau} x_0 \tag{2}$$

K_{F0} is proportional coefficient that depends on effective airgap length as well as design parameters of both the stator and the AEM. J_1 is the amplitude of the equivalent surface-current density produced by the armature current I_1. The fundamental equivalent volume-current density J_{C1} is produced by AEM current I_2. Details of J_1 and J_{C1} calculations can be found in [5]. x_0 is the mechanical load angle.

The levitation force developed by the AEM has two main components. First, the attractive force between the AEM and the stator back iron F_{zM}. Second the attractive or repulsive force between the AEM and the starter current carrying windings F_{zMS}, which depends on the mechanical load angle x_0. Hence, the AEM levitation force F_{zAEM} is given by:

$$F_{zAEM} = F_{zM} + F_{zMS} \tag{3}$$

where

$$F_{zM} = K_{zM} J_{C1}^2 \tag{4}$$

$$F_{zMS} = K_{zMS} J_1 J_{C1} \cos\frac{\pi}{\tau} x_0 \tag{5}$$

Similarly, the coefficients K_{zM} and K_{zMS} are depend on the effective airgap length and design parameters of the primary and AEM coils.

It is obvious from equations (2-5) that F_{xAEM} and F_{zAEM} are functions of J_{C1}. Therefore, the DC current fed to the electromagnet coils could be used to actively control the pitching motion.

From simple geometry as shown in Fig.4, the torque developed by one AEM is given by:

$$\begin{aligned} T_{AEM} &= F_{zAEM}(d\sin\phi - L_{AEM}\cos\phi) \\ &\quad - F_{xAEM}(d\cos\phi + L_{AEM}\sin\phi) \end{aligned} \tag{6}$$

where d and L_{AEM} are the vertical and horizontal distances between the center of the AEM and the ME02's center of gravity. L_{AEM} was chosen in a manner that maximizes the developed torque in order to reduce the current. L_{AEM} was taken as a multiple of the pole pitch distance τ to minimize the effects of the AEM on the thrust and lift forces developed by the PM-LSM of ME02. It is notable that both the AEM and PM-LSM will have the same load angle. Under the physical design restrictions and simulation results, the number of AEM coil turns N_2 has been found to be optimally 100 turns.

Fig.5 shows the variation of trust force, lift force and developed torque against load angle for different currents. Both positive and negative currents are presented to state clearly that the AEM is able to produce both attractive and repulsive toques. It is clear that, the at-

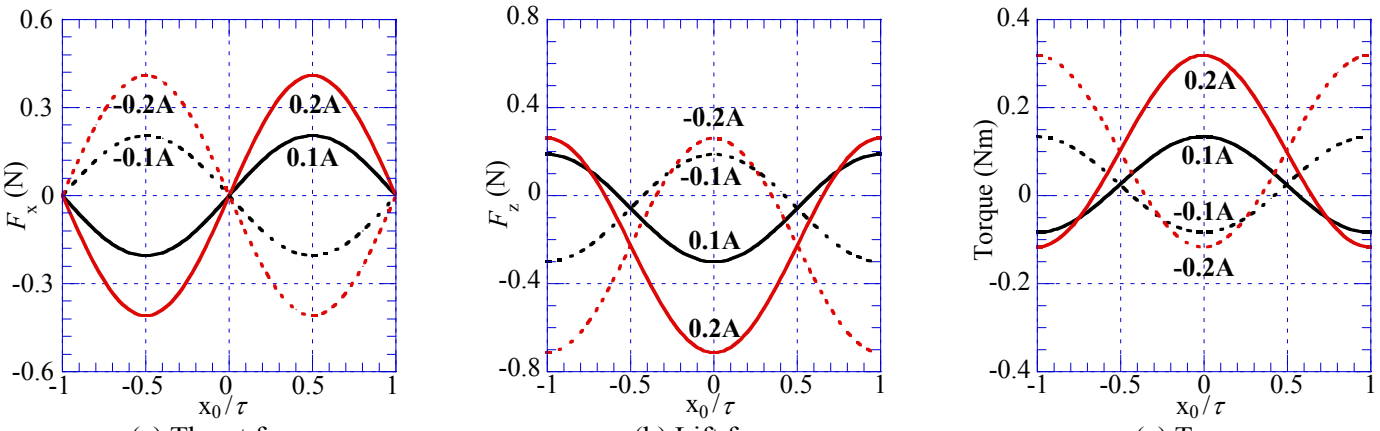

(a) Thrust force (b) Lift force (c) Torque

Fig.5 Characteristics of AEM

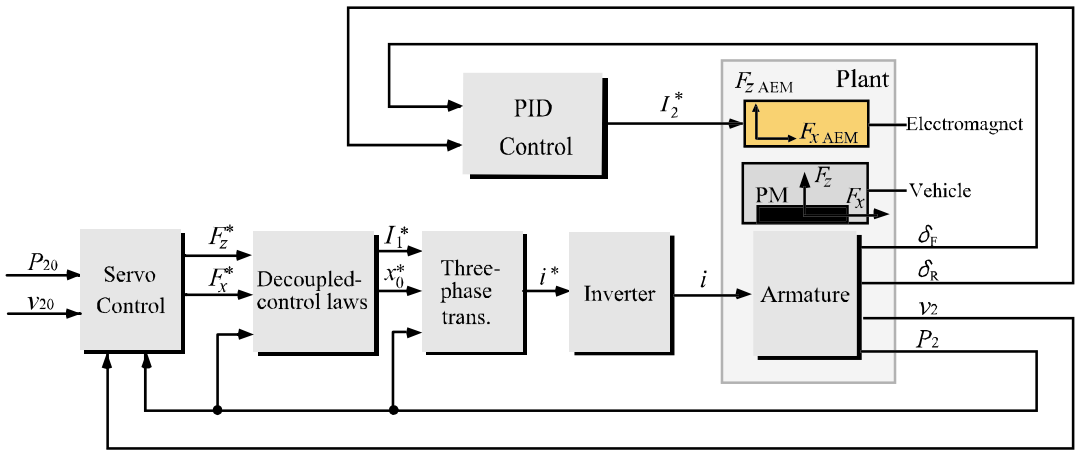

Fig.6 Control system with pitching motion control

tractive torque rotating towards the guideway will require smaller current. To extend the control flexibility, two AEM are proposed in the front and rear of the vehicle. The control principle will be provided in the next section.

4 Proposed Control Scheme

The ME02 propulsion motion in *x*-direction and levitation motion in z-direction are supposed to follow a desired motion demand pattern. It describes the demand position $P_{20}(x_{20}, z_{20})$ and demand speed $v_{20}(v_{x20}, v_{z20})$. According to the actual vehicle position $P_2(v_{x2}, v_{z2})$, vehicle speed $v_2(v_{x2}, v_{z2})$ and the required motion demand pattern, the new command forces F_x^*, F_z^* are determined using servo PID controller. Based on the decoupled control law, the command armature current and command load angle are obtained [6]. The obtained values are used to determine the command three phase instantaneous current i^*, which in turn controls three phase inverter. Hence, instantaneous three phase current i is applied to the armature windings. The traveling magnetic wave generated by the armature winding enforces the vehicle to move to its new position.

As the AEM coil is placed on a distance that is a multiple of PM-LSM pole pitch, the load angle obtained from the decoupled control law is the same for both AEM and PM-LSM. Hence, based on the front and rear airgap values, the front and rear AEM currents can be found as follows:

$$I_2^* = K_P(\phi_0 - \phi) + K_I\int(\phi_0 - \phi)dt + K_D(\omega_0 - \omega) \qquad (7)$$

where K_P, K_I and K_D are proportional-integral-derivative gains in order. The actual and demand pitching speed around *y*-axis are ω and ω_0 respectively. The demand pitching angle ϕ_0 is zero for horizontal motion.

The pitching angle ϕ is given by the following equation:

$$\phi = -\sin^{-1}\left(\frac{\delta_F - \delta_R}{2L_R}\right) \qquad (8)$$

where L_R is the horizontal distance between the airgap sensors and the vehicle center of gravity.

5 Simulation results and discussion

A simulated study has been performed to investigate the effectiveness of the proposed pitching motion control scheme. As mentioned before, the motion of the ME02 is supposed to follow a certain demand pattern.

In Fig.7(a) and Fig.7(b) the vehicle demand and simulated trajectories for both position and speed are shown. The torque developed by the PM-LSM is shown in Fig.7(c), which leads to the existence of pitching motion. According to the demand pattern, the airgap length is 9 mm. In Fig.7(d) the variation of effective airgap length at the center of the vehicle shows that a good tracking for the demand pattern is achieved. However, some disturbances exist because the difference between the front and rear airgap lengths. Such difference is shown in Fig.7(e). As stated earlier, this difference is mainly taking place due to the resultant torque developed by motor forces. In Fig.7(f), the pitching angle is represented. Hereby, the importance of pitching motion control is clarified.

Fig.8 shows the simulated dynamics when applying pitching motion control. In Fig.8(a) and Fig.(b) the demand and simulated vehicle position and speed are shown. In comparison with Fig.7, it is clear that the AEM coils have negligible effect on the PM-LSM performance. On the other hand, Fig.8(c), Fig.8(d) and Fig.8(e) show the effective airgap, font and rear airgap, and the resultant pitching angle. It is obvious that the maximum pitching angle is reduced from 0.38° to 0.0008°. That clarifies the effectiveness on the proposed scheme. Fig.8(f) and Fig.8(g) represent the AEM propulsion force F_{xAEM} and levitation force F_{zAEM} respectively. The front and rear coil developed torques in comparison with the PM-LSM one are shown in Fig.8(h). It is clear that the two coils almost equally share the compensation of the PM-LSM torque.

Fig.8(i) shows the AEM coil current with maximum value of 35mA. In consequence to the small current required, the copper loss is reduced one third as compared

with that of using single coil. The variation of power loss is shown in Fig.8(j).

6 Conclusion

In the current work, a new pitching motion control scheme for Marine Express using 2 air-cored electromagnets has been applied to the underwater linear motor vehicle ME02. Also, the design and operation details have been introduced. A simulated study has been performed. The pitching motion has been successfully damped in more effective way than previously proposed methods. Moreover, the required control current is relatively smaller than previously proposed air-cored electromagnet control for pitching motion. The proposed scheme shows its validity for application in real size Marine Express.

References:

[1] K. Yoshida, H. Muta and N. Teshima, "Underwater linear motor car", *International Journal of Applied Electromagnetics in Materials*, 1991, pp. 275-280.

[2] K. Yoshida, L. Shi and H. Takami, "Attractive-Mode Levitation and Propulsion of an Underwater Traveling Marine-Express Model Vehicle ME02", *Proc. of ICEMA'96 Harbin,* 1996, pp. 171-174.

[3] K. Yoshida, L. Shi and H. Takami, "Pitching-motion control of underwater traveling ME02 in repulsive-mode", *National Convention Record IEE. Japan*, No. 1202, 1997

[4] K. Yoshida, A. Nafa and Y. Nakamura, "Pitching Motion Control in Attractive Levitation Using Controlled Electromagnet", *7th International Symposium on Magnetic Suspension Technology*, *Fukuoka, Japan*, 2003, pp.320-327

[5] K. Yoshida and H. Weh, "Theory of a controlled-PM linear synchronous motor", *Tenth International Conference on Magnetically Levitated Systems (Maglev), Congress Centrum Hamburg, Federal Republic of Germany*, 1988, pp. 259-268

[6] K. Yoshida, H. Takami and L. Shi, "Decoupled-control method for levitation and propulsion in amphibious train marine-express", *Memoirs of the Faculty of Engineering, Kyushu University*, Vol. 55, No. 4, 1995, pp. 467-489

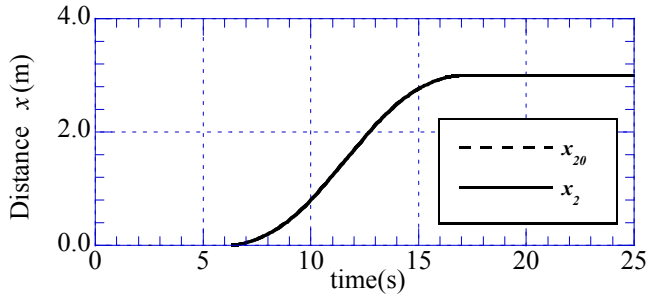

(a) Demand and simulated vehicle position

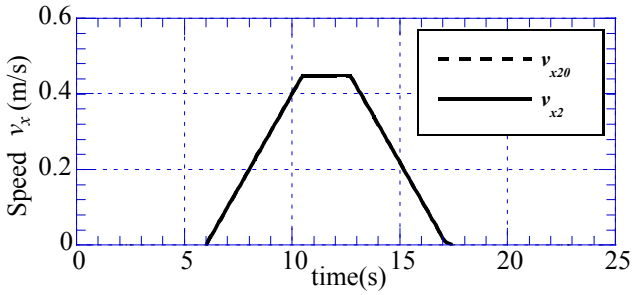

(b) Demand and simulated vehicle speed

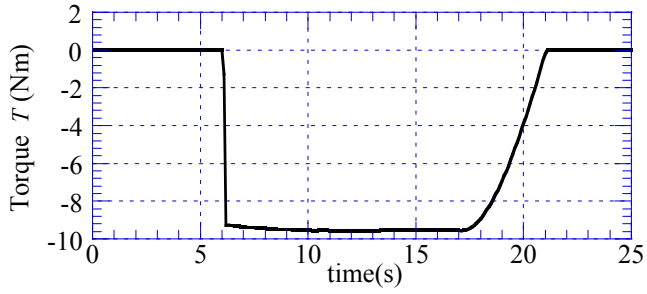

(c) PM-LSM developed torque

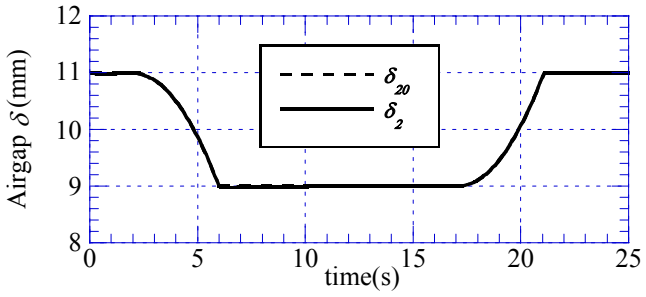

(d) Demand and simulated effective airgap length

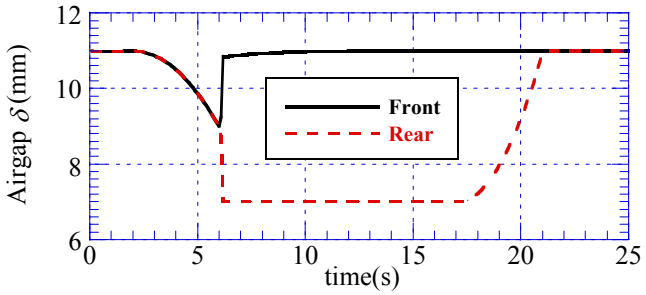

(e) Front and rear airgap lengths

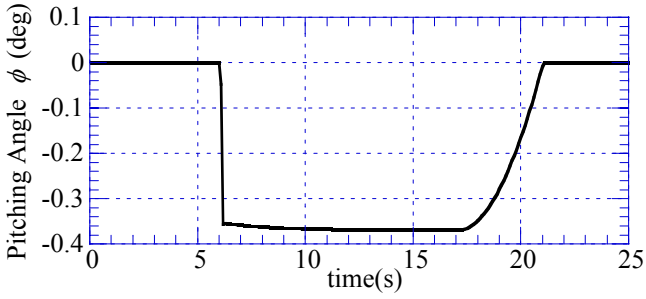

(f) Pitching angle

Fig.7 Results of ME02 dynamics simulation without pitching control

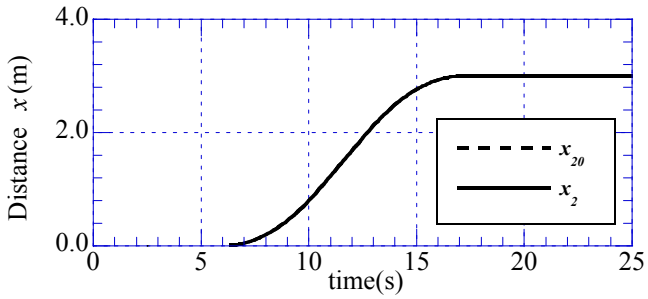

(a) Demand and simulated vehicle position

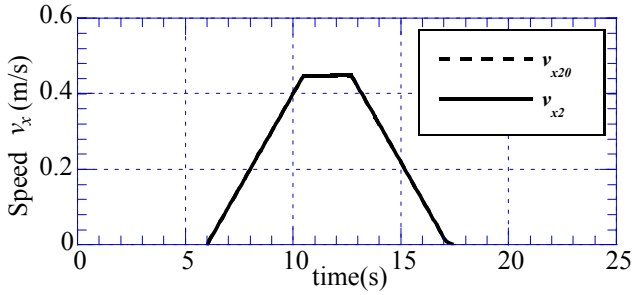

(b) Demand and simulated vehicle speed

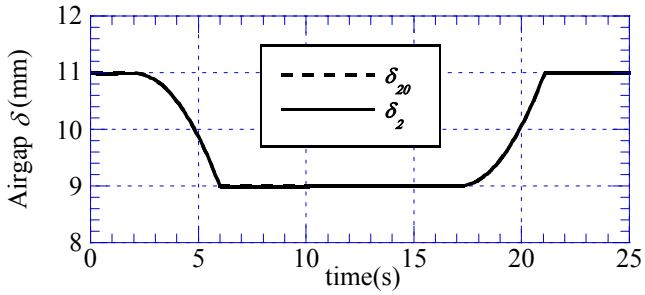

(c) Demand and simulated effective airgap length

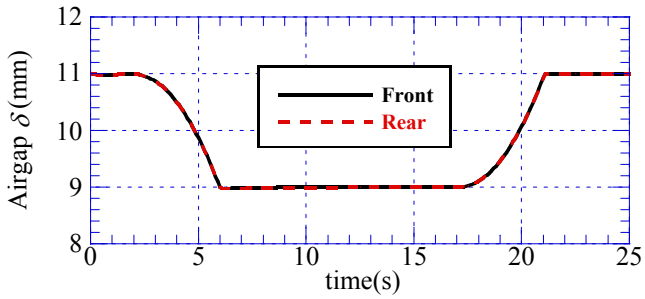

(d) Front and rear airgap length

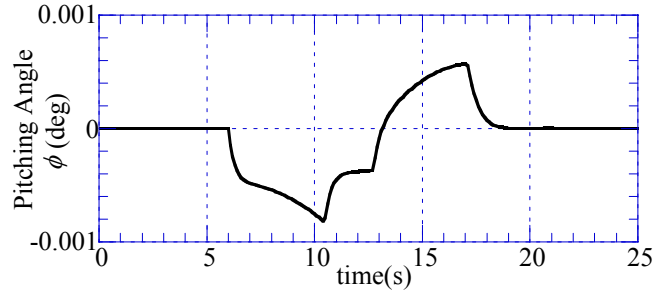

(e) Pitching angle

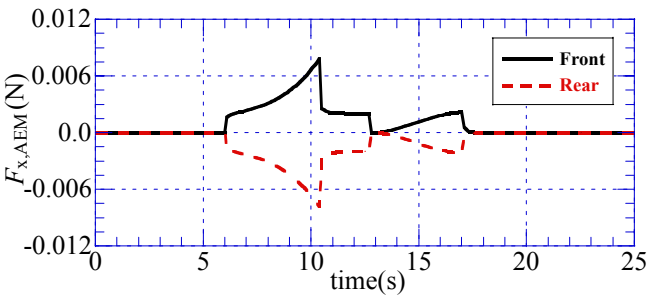

(f) AEM propulsion force

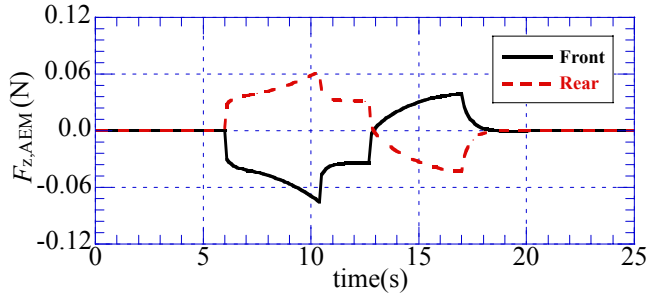

(g) AEM levitation force

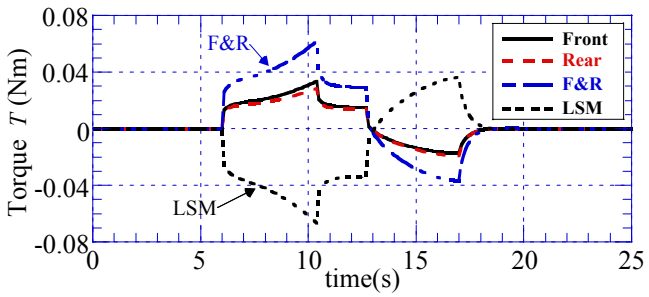

(h) Developed torques

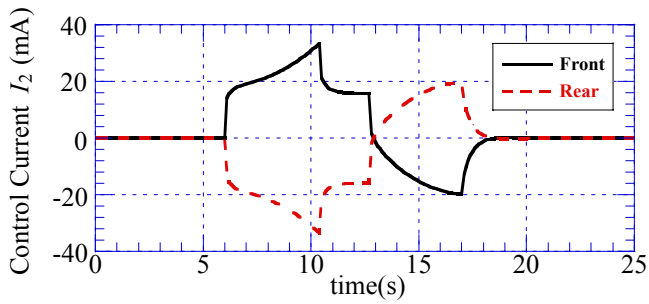

(i) AEM current

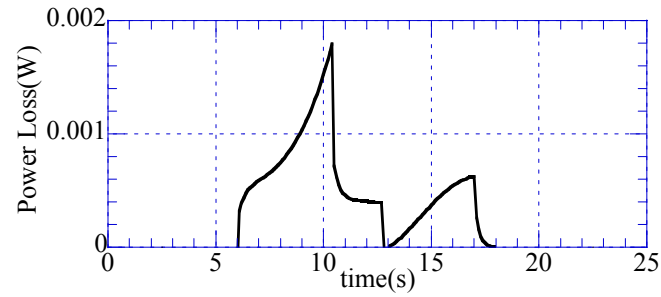

(j) Total AEM coils power loss

Fig.8 Results of ME02 dynamics simulation with pitching control